Development 139, 2288-2298 (2012) doi:10.1242/dev.078071

The developmental dismantling of pluripotency is reversed by ectopic Oct4 expression

Rodrigo Osorno[1,*], Anestis Tsakiridis[1,*], Frederick Wong[1], Noemí Cambray[1], Constantinos Economou[1], Ronald Wilkie[1], Guillaume Blin[1], Paul J. Scotting[2], Ian Chambers[1,‡] and Valerie Wilson[1,‡]

SUMMARY

The transcription factors Nanog and Oct4 regulate pluripotency in the pre-implantation epiblast and in derivative embryonic stem cells. During post-implantation development, the precise timing and mechanism of the loss of pluripotency is unknown. Here, we show that in the mouse, pluripotency is extinguished at the onset of somitogenesis, coincident with reduced expression and chromatin accessibility of *Oct4* and *Nanog* regulatory regions. Prior to somitogenesis expression of both Nanog and Oct4 is regionalized. We show that pluripotency tracks the in vivo level of Oct4 and not Nanog by assessing the ability to reactivate or maintain Nanog expression in cell culture. Enforced Oct4 expression in somitogenesis-stage tissue provokes rapid reopening of *Oct4* and *Nanog* chromatin, Nanog re-expression and resuscitates moribund pluripotency. Our data suggest that decreasing Oct4 expression is converted to a sudden drop in competence to maintain pluripotency gene regulatory network activity that is subsequently stabilized by epigenetic locks.

KEY WORDS: Pluripotency, Mouse embryo, Oct4, Nanog, Teratocarcinoma, Transcription factor, Chromatin, Somitogenesis

INTRODUCTION

During early embryonic development, cells have the capacity to form derivatives of all three embryonic germ layers, a property known as pluripotency. In the environment of the early embryo, pluripotent founder cells respond to patterning signals to differentiate appropriately. However, following grafting to permissive sites, such as the adult kidney capsule in the mouse, all known pluripotent cell types seed teratomas – tumours containing a chaotic mixture of differentiated derivatives of the three embryonic germ layers. A major subset of these, termed teratocarcinomas, also contain self-renewing embryonal carcinoma (EC) cells and are consequently malignant (Andrews, 2002; Solter, 2006). In newborn humans, the rare spontaneous incidence of teratomas and teratocarcinomas along the midline from the forebrain to the base of the spine suggests that developmental suppression of pluripotency normally prevents occurrence of these tumours (Oosterhuis and Looijenga, 2005). Previous analyses have shown that teratocarcinoma-forming potential is lost in mouse during the broad developmental period from ~E7.5 to ~E8.5 (Damjanov et al., 1971).

Pluripotency during pre-implantation development and in embryonic stem (ES) cells is governed by a gene regulatory network centred on the core transcription factors Oct4, Sox2 and Nanog (Avilion et al., 2003; Chambers et al., 2007; Masui et al., 2007; Mitsui et al., 2003; Nichols et al., 1998; Niwa et al., 2000; Silva et al., 2009) (reviewed by Chambers and Tomlinson, 2009). Oct4, Sox2 and Nanog are also expressed in the pluripotent post-implantation epiblast and in derivative epiblast stem cell (EpiSC) lines (Brons et al., 2007; Tesar et al., 2007). Classical teratogenesis experiments showed that pluripotency persists in the epiblast at E7.5 but is lost a full day later (Beddington, 1983; Damjanov et al., 1971). However, the role of Oct4, Sox2 and Nanog in the pluripotency of post-implantation embryos or EpiSCs has never been defined.

Here, we determine the precise time at which somatic cells cease to be pluripotent during embryonic development. We correlate this loss of pluripotency with changes occurring in the expression of Oct4 and Nanog. Closure of the regulatory elements of the *Nanog* and *Oct4* genes contributes to this loss of pluripotency. An initial period during which pluripotency can be rapidly reinstated by enforcing Oct4 expression is followed by stable epigenetic repression of pluripotency factor genes.

MATERIALS AND METHODS

Mouse husbandry, staging, culture and micromanipulation of embryos

Mice were maintained on a 12-hour light/12-hour dark cycle. For timed matings, noon on the day of the vaginal plug was designated E0.5. Except where stated, wild-type strains were MF1 or 129/Ola. Gastrulation-stage embryos were staged as described (Downs and Davies, 1993): ES, early streak; MS, mid-streak; LS, late streak; OB, no allantoic bud; EB, early allantoic bud; LB, late allantoic bud; EHF, early headfold; LHF, late headfold.

Embryos were cultured in static 4-well dishes in an incubator at 5% CO_2 in air in 50% rat serum as described (Copp, 1990). Blastocyst injection and embryo transfer was performed using standard procedures.

Ubiquitously induced Oct4 expression was achieved by crossing wild-type females with homozygous males carrying both the doxycycline-inducible reverse tet transactivator (rtTA) targeted at *Rosa26* and a doxycycline-responsive Oct4 transgene (*TgOct4)* targeted at *Col1a1* [B6;129-Gt(ROSA)26Sor$^{tm1(rtTA*M2)Jae}$ Col1a1$^{tm2(tetO-Pou5f1)Jae/J}$ (Hochedlinger et al., 2005)].

Dissection of tissues for grafting, explant culture and expression analysis

Wild-type (C57BL/6, 129 and CBA) embryo subregions were dissected in M2 (Sigma) as described (Cambray and Wilson, 2007). To dissect distal/anterior (Nanog:GFP negative) and proximal/posterior (Nanog:GFP

[1]Institute for Stem Cell Research, MRC Centre for Regenerative Medicine, School of Biological Sciences, University of Edinburgh, 5 Little France Drive, Edinburgh EH16 4UU, UK. [2]Children's Brain Tumour Research Centre, Institute of Genetics, University of Nottingham, Queen's Medical Centre, Nottingham NG7 2UH, UK.

*These authors contributed equally to this work
‡Authors for correspondence (ichambers@ed.ac.uk; v.wilson@ed.ac.uk)

Accepted 25 April 2012

positive) regions of the E7.5 embryo, embryos were first ordered relative to developmental stage and imaged to assess GFP-positive and -negative regions. A transverse cut was made to separate the most proximal epiblast, containing primordial germ cells, together with the extra-embryonic region, from the distal epiblast. A second cut was made to separate the distal/anterior from posterior/proximal regions. Finally, the embryos were viewed with fluorescence optics to check the accuracy of microdissection; any remaining Nanog-GFP-positive cells were trimmed from distal-anterior regions. To dissect prospective forebrain (region 1) and adjacent region (region 2), extra-embryonic membranes were removed and the embryo laid flat dorsoventrally, with the aid of a transverse cut near the node if necessary (see Fig. 5). Forebrain and adjacent region were then separated with glass needles.

Teratocarcinoma assays

Kidney capsule grafts were performed as described (Tam, 1990), except that transfer to NOD/SCID mice was performed in a laminar flow cabinet. After transplanting E8.5 *TgOct4/+;rtTA/+* forebrains, half of the host animals were administered 1 mg/ml doxycycline (Sigma) through the drinking water for 4 weeks. Tumours were recovered at 4-6 weeks and fixed in 4% paraformaldehyde (PFA) for 1-7 days depending on tumour size. Tissue was processed and stained as described (Bancroft and Gamble). Tissues representative of different germ layers used for scoring all tumours are shown in supplementary material Fig. S2.

Explantation and culture of EpiSC

To derive E7.5-E8.0 (OB-2s) EpiSC lines, embryos were dissected, dissociated (without removal of endoderm or mesoderm) and explanted into EpiSC medium (Tesar et al., 2007) supplemented with 20 ng/ml activin-A (PeproTech) and 10 ng/ml bFGF (R & D) and plated on irradiated mouse embryo fibroblasts (MEFs). After 2-3 days, primary explants were passaged by incubation with 1× accutase (Sigma, Catalogue number A 6964) (5 minutes) and then triturated into 10- to 100-cell clumps, neutralized with EpiSC medium and replated. Subsequent passages were performed every 5-6 days. Cultures were designated as cell lines when they had reached passage 3, exhibiting EpiSC morphology and robust proliferation.

TgOct4-overexpressing explants and EpiSCs were derived from *TgOct4/TgOct4;rtTA/rtTA* homozygous male crossed with either 129/Ola wild-type or Nanog:GFP [129-Nanog$^{tm1(GFP-IRES-Puro)}$] females, derived from TNG targeted ES cells (Chambers et al., 2007). Medium was initially supplemented with 1 mg/ml doxycycline, and reduced to 0.5 mg/ml after three passages. *Nanog*$^{-/-}$ EpiSCs were derived in vitro from ES cells as described (Guo et al., 2009) and passaged in accutase as above. Oct4GiP EpiSCs were derived from ES cells carrying an Oct4-promoter driven eGFPiresPuroR-polyA transgene (Ying et al., 2002). When added, chemical inhibitors were used at these concentrations: PD0325901 (Stemgent), 1 μM; SB 431542 (Sigma), 10 μM; JAK inhibitor I (Calbiochem 420099), 0.6 mM.

Teratocarcinoma-derived secondary EpiSCs

Tumours were isolated and chopped roughly before dissociation in 0.5% trypsin/2.5% pancreatin in PBS (37°C, 15 minutes). After trituration, cells were plated onto irradiated MEFs in EpiSC media, passaged the next day and then every 2-3 days.

RNA analysis

Total RNA (30 ng-1 μg) isolated using the RNeasy microkit or minikit (Qiagen), was used for cDNA synthesis using SuperScript III (Invitrogen). Quantitative PCR was performed using Light Cycler 480 SYBR Green I Master Mix (Roche). PCR primer sequences are available on request. Values for each gene were normalized to expression of TATA-box binding protein (TBP) and expressed as mean±s.e.m. of at least three replicates, relative to ES cell levels.

Immunohistochemistry and immunocytochemistry

Whole embryos or cultured cells were fixed using 4% PFA in PBS for 2 hours (embryos) or 10 minutes (cells) at 4°C followed by permeabilization in 0.5% Triton X100 (Sigma) in PBS for 15 minutes. Samples were incubated in 1 M glycine in PBS/0.1% TritonX100 (PBST) for 20 minutes and blocked overnight at 4°C using 3% serum (Sigma), 1% BSA (Sigma) in PBST. Primary antibodies were diluted in blocking buffer to the working concentrations indicated below and applied for 1-2 hours at room temperature (cells) or 48 hours at 4°C (embryos). After three (cells) or four to six (embryos) PBST washes (15 minutes at room temperature), Alexa-conjugated secondary antibodies (Molecular Probes; 2 μg/ml in blocking buffer) were applied for 1 hour (cells) or 3 hours (embryos) in the dark at room temperature. Cells/embryos were then washed at least three times in PBST followed by incubation in 4′,6-diamidino-2-phenylindole (DAPI) to stain nuclei. Primary antibody concentrations were: Nanog, 1.4 μg/ml (Chambers, 2004) (embryos) or 2.5 μg/ml (ab14959, Abcam) (cells); Oct4, 1 μg/ml (Santa Cruz, N-19) (embryos) or 1 μg/ml (Santa Cruz, C-10) (cells); Sox2, 1 μg/ml (Santa Cruz, Y-17) (cells).

In situ hybridization

Whole-mount in situ was performed as described (Wilkinson et al., 1990); proteinase K treatment was empirically adjusted between 8-16 minutes according to embryo size and stage. The riboprobes used were: *Oct4* (Scholer et al., 1990) and *Nanog* (Chambers et al., 2003). Embryos were sectioned in paraffin wax (7 μm).

Imaging

Images were captured using Volocity (Improvision) software on a Zeiss Stemi SV11 dissecting microscope (for whole embryos), an Olympus IX51 (for cultured cells), or an Olympus BX61 (for sections). Image processing was performed using Adobe Photoshop software. In the case of whole embryos stained with Oct4, fluorescence was visualized using a Leica DM IRE2 inverted confocal microscope (Leica Microsystems). Image acquisition and processing were carried out using the Leica Confocal (Leica Microsystems) and Volocity (Improvision) software packages, respectively.

Image analysis

To quantify fluorescence signal per nucleus, we generated a semi-automated image analysis pipeline. Regions of interest in embryos were cropped and analysed in parallel with an internal negative control region (supplementary material Fig. S5). These RGB images were pre-processed [background subtraction in each channel and gamma correction in the blue channel (DAPI) to enhance weakly fluorescing nuclei] using our own plug-in in ImageJ (http://rsbweb.nih.gov/ij/). To distinguish individual nuclei, the blue channel was segmented using a previously published algorithm (Li et al., 2007) with the following parameters and their respective values for 2D and 3D images: sigma 0.1 (2D);0.15 (3D), minimum nucleus size 350 pixels (2D and 3D), and fusion threshold 2 (2D);1 (3D); see supplementary material Fig. S5). In the resulting image, each nucleus is labelled with a unique greyscale-based identifier. Using a Java application that we developed within eclipse (www.eclipse.org), average pixel intensities in the red and green channels of the preprocessed RGB image were calculated within the superimposed volume of each nucleus. Charts representing red and green average intensities were generated using the Jfreechart library (http://www.jfree.org/jfreechart/). Applications developed for this analysis can be downloaded at http://www.crm.ed.ac.uk/research/group/embryonic-stem-cell-differentiation.

DNA methylation analysis

Bisulphite sequencing was performed using the Imprint DNA modification kit (Sigma) together with primers meNanog-F2-S and meNanog-F2-AS (Imamura et al., 2006). Approximately 30 clones were sequenced; sequences characterized by incomplete bisulphite conversion were discarded.

Formaldehyde-assisted isolation of regulatory elements (FAIRE)

MEFs or E14Tg2a cells (1×10^7) were used. MF1 embryos, staged as described previously (Downs and Davies, 1993) were dissected free of extra-embryonic tissue (including the allantois containing primordial germ cells). Embryos were pooled [for E7.5 (LB-EHF), 27-30 embryos; for E8.5 (2-8 somites), 20-22 embryos] and dissociated in 0.5% trypsin/2.5% pancreatin/PBS. For E8.5 explants, 20-22 dissociated embryos were

cultured in EpiSC conditions with or without 1 mg/ml doxycycline. After 24 hours, explants were trypsinized, replated on non-gelatinized tissue culture dishes for 15 minutes to deplete feeders and collected.

Formaldehyde-crosslinked, sonicated chromatin was prepared as previously described (Navarro et al., 2010) and 20 μg used to prepare FAIRE and reference samples. For the FAIRE sample, protein-free DNA molecules of the crosslinked chromatin were purified by phenol-chloroform extraction and ethanol precipitated as described previously (Giresi et al., 2007). For the reference sample, crosslinking was reversed by overnight incubation at 65°C in TE/1% SDS, phenol-chloroform extracted and ethanol precipitated. FAIRE and reference samples were analysed in parallel using a LightCycler 480 (Roche) and LightCycler 480 SYBR Green 1 Master (Roche). Primer sequences were: Nanog, TGGCCTTCAGATAGGCTGAT (sense) and CAAGAAGTCAGAAGGAAGTGAGC (antisense); Sox2, AGGGCTGGGAGAAAGAAGAG (sense) and CCGCGATTGTTGTGATTAGTT (antisense); Oct4 distal enhancer AGAGTGCTGTCTAGGCCTTA (sense) and CCAGAACTCTCAACCTCCCT (antisense); Oct4 proximal enhancer, GGGAAGCAGGGTATCTCCAT (sense) and TCCCCTCACACAAGACTTCC (antisense).

RESULTS

Decline of Nanog and Oct4 expression during embryonic development

To examine the relationship between loss of pluripotency and expression of core pluripotency regulators, quantitative RT-PCR (qPCR) was performed on RNA from whole embryos throughout the period covering the reported disappearance of pluripotency (Damjanov et al., 1971). Owing to the natural variation in developmental stage between littermates, precise assessment of the stage of embryo development was made using the morphological criteria of Downs and Davies (Downs and Davies, 1993) (Fig. 1). Expression of Sox2 [which continues in developing neurectoderm (Avilion et al., 2003)] increases throughout this period, whereas Nanog and Oct4 expression declines, becoming undetectable in the somatic cells of three- to five-somite embryos (Nanog) and 12- to 15-somite embryos (Oct4) (Fig. 1A; supplementary material Fig. S1).

A period of developmental plasticity in Nanog expression marks pluripotency

The temporal correlation between the reported loss of pluripotency and Nanog expression prompted further analysis of its spatiotemporal expression pattern. As judged by immunofluorescence, in situ hybridization and GFP reporter expression from the endogenous *Nanog* gene (Chambers et al., 2007) (Fig. 1B; supplementary material Fig. S1A), Nanog is strongly expressed in the proximal-posterior region from the start of gastrulation, consistent with published data (Hart et al., 2004; Hatano et al., 2005). Expression is lost as cells delaminate to move through the primitive streak (supplementary material Fig. S1A). Nanog is excluded from the distal/anterior epiblast (Fig. 1B; supplementary material Fig. S1A,B) and subsequently disappears entirely from the epiblast at the onset of somitogenesis. Expression is re-established in primordial germ cells (PGCs), as documented previously (Chambers et al., 2003; Yamaguchi et al., 2005). In the embryo proper, the last detectable expression of GFP is localized to the distal tip at 0-1 somites (Fig. 1B). This region was therefore tested for pluripotency from headfold to early somite stages. Kidney capsule grafts from presomite embryos produced large teratocarcinomas containing derivatives of all three germ layers and EC cells (two out of four tumours were teratocarcinomas), consistent with published data (Beddington, 1983) (Fig. 1C; supplementary material Fig. S2). However, the equivalent tissue from two- to five-somite embryos produced small growths devoid of EC cells and endoderm (n=23) (Fig. 1C). qPCR analysis of the distal tip at two to five somites revealed expression of Oct4 and Sox2, but confirmed that Nanog transcripts were absent

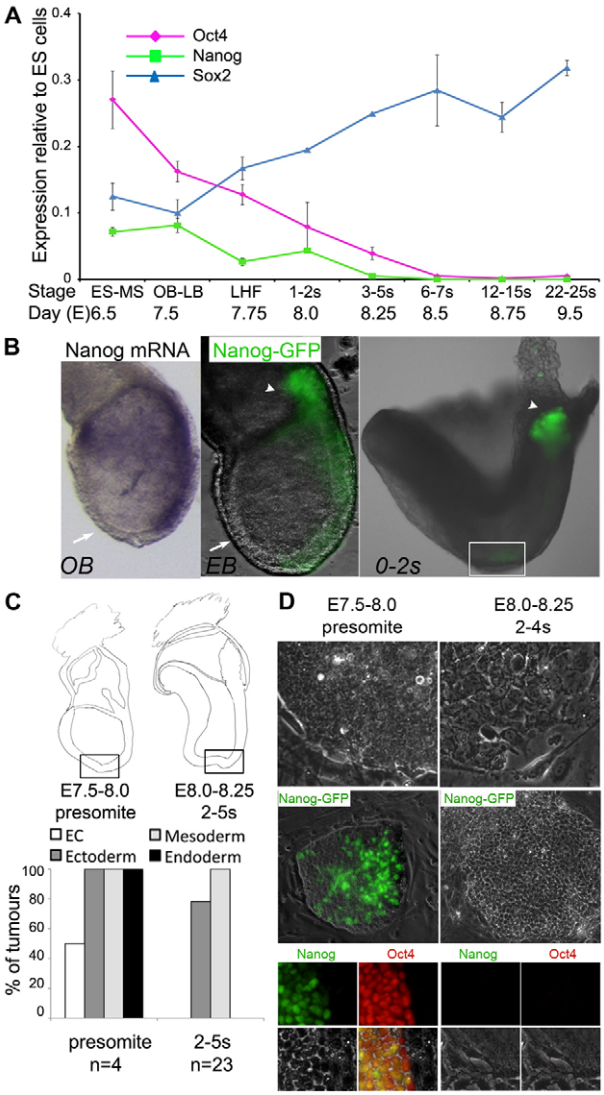

Fig. 1. Pluripotency disappears from the epiblast as *Oct4* and *Nanog* levels decline. (**A**) qPCR analysis of *Oct4*, *Nanog* and *Sox2* mRNAs in pooled embryos. Pre-somitogenesis embryos were staged as described previously (Downs and Davies, 1993). ES, early streak; MS, mid-streak; OB, no allantoic bud; LB, late allantoic bud; LHF, late headfold. In later stage embryos, embryos are staged by number of somite pairs (s); approximate embryonic day (E) is indicated. qPCR data in all figures are normalized to embryonic stem cell levels. Error bars indicate ±s.e.m. of three biological replicates. (**B**) Nanog mRNA and Nanog:GFP expression. Arrow indicates distal-anterior region lacking Nanog. EB is early allantoic bud. Arrowheads indicate primordial germ cells. Box indicates distal region showing residual Nanog:GFP. (**C**) Teratocarcinoma-forming capacity of distal regions (boxed). Tissues used to score germ layers are shown in supplementary material Fig. S2. (**D**) Ability of E7.5-E8.25 embryos to form EpiSC, as assayed by EpiSC colony morphology (top), expression of Nanog:GFP (middle) and immunoreactivity to Nanog and Oct4 (bottom).

(supplementary material Fig. S1E). Therefore, pluripotency disappears at early somitogenesis, coincident with extinction of Nanog but before Oct4 becomes undetectable.

We next investigated the concordance of EpiSC derivation and teratocarcinoma formation. EpiSC lines have previously only been derived up to E6.5 (Brons et al., 2007). Upon explantation of tissue from E7.5-E8.0 pre-somite embryos in EpiSC conditions, Nanog:GFP was readily detected in explants. These explants could be passaged and in all cases (8/8) gave rise to EpiSC lines that expressed Oct4 and Nanog protein (Fig. 1D). By contrast, explants from two- to four-somite embryos did not express Nanog:GFP (0/6). Upon passaging, these explants produced morphologically differentiated cells that did not express Oct4 or Nanog (Fig. 1D). Thus, the ability to derive EpiSC lines is lost concomitant with the loss of teratocarcinoma-forming potential, indicating that EpiSC derivation is an effective assay for post-implantation pluripotency.

To examine the relationship between pluripotency and Nanog expression in more detail, a staged series of *Nanog:GFP* embryos was isolated, separated into distal/anterior (Nanog-nonexpressing) and proximal/posterior (Nanog-expressing) regions, and explanted in EpiSC culture conditions (Fig. 2). The presence of bright GFP-positive PGCs at the base of the allantois allowed us to confirm exclusion of these cells from posterior explants. Without exception, prior to somitogenesis, anterior and posterior explants showed Nanog expression at 24-48 hours (Fig. 2A) and produced stable EpiSC lines expressing characteristic markers (n=12 for each; Fig. 2D,E; supplementary material Fig. S3C). Levels of marker expression in all EpiSC lines tested in the present work were within the limits of variation observed previously for EpiSC lines (Brons et al., 2007; Guo and Smith, 2010; Guo et al., 2009; Hayashi and Surani, 2009). In addition, prior to somitogenesis, anterior and posterior explants showed equivalent teratocarcinoma-forming capacity (three out of four anterior versus six out of nine posterior-derived tumours were teratocarcinomas; supplementary material Fig. S3A,B). In striking contrast, not a single explant from embryos that had initiated somitogenesis, including the two late headfold stage embryos shown in Fig. 2B, where somitogenesis is incipient, reactivated *Nanog* or formed EpiSC lines, from anterior or posterior tissue (0/11 of each). In total, 23 EpiSC lines from presomitogenesis-stage embryos were established and passaged three to nine times (supplementary material Table S1). No lines were isolated from somite-stage embryos (n=21). Therefore, there is a dramatic drop in pluripotency that occurs simultaneously in anterior and posterior tissue between headfold and somitogenesis stages. Together, these results indicate that Nanog re-expression in vitro correlates with EpiSC derivation and teratocarcinoma formation, and thus with pluripotency. Furthermore, the ability of cells to activate Nanog expression within 24 hours of explantation in EpiSC conditions (Fig. 2A) demonstrates plasticity of gene expression within the anterior epiblast at this stage.

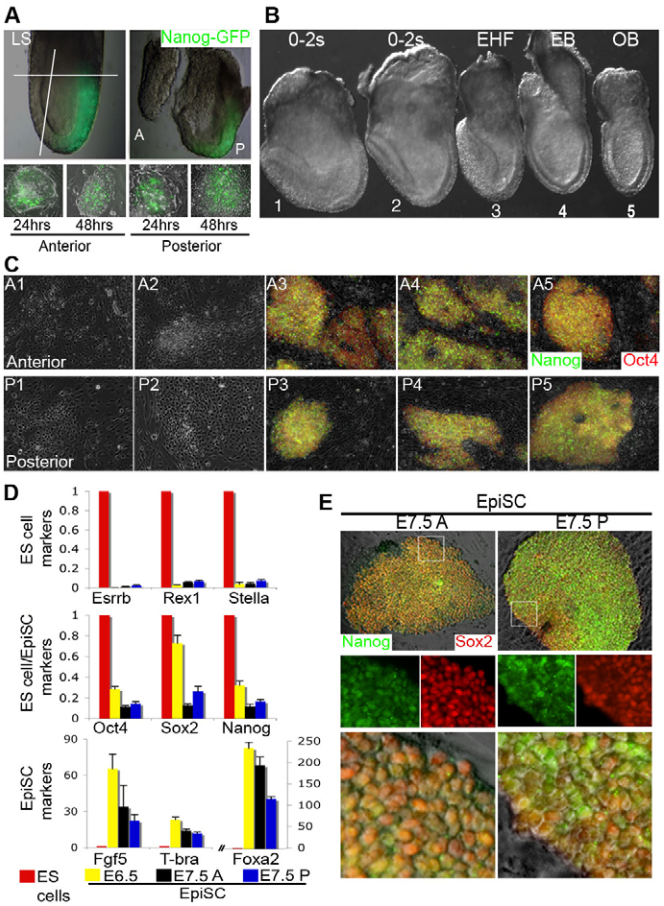

Fig. 2. Pluripotency disappears at the onset of somitogenesis and is equivalent in Nanog-negative and Nanog-positive epiblast. (**A**) E7.5 embryos expressing Nanog:GFP (green) were dissected into anterior (A) and posterior (P) fragments (indicated by lines). Bottom shows Nanog:GFP expression upon explantation. LS, late streak. (**B**) Embryos before microdissection, arranged from oldest (left) to youngest (right). EHF, early headfold stage; EB, early allantoic bud; OB, no allantoic bud. (**C**) Oct4 and Nanog immunofluorescence in representative colonies of EpiSC lines derived from these embryos. A1-5 and P1-5 are lines derived from anterior and posterior fragments of numbered embryos in B. (**D**) qPCR of representative anterior and posterior E7.5 EpiSC lines compared with an E6.5 EpiSC line. Data are mean±s.e.m. (**E**) Nanog and Sox2 immunofluorescence in representative anterior and posterior EpiSC lines. Box in top panels: region magnified below. Note that Nanog expression is reproducibly more heterogeneous than Oct4 or Sox2.

Nanog is not required for post-implantation pluripotency

Two possibilities may explain the observation that Nanog-nonexpressing epiblast cells are pluripotent prior to somitogenesis. Either these cells represent a latent pluripotent state that requires Nanog reactivation to manifest pluripotency, or Nanog is not essential for epiblast pluripotency. To distinguish between these possibilities, *Nanog*$^{-/-}$ ES cells were used to produce E6.5-E7.5 chimaeras (Fig. 3A,B), which were then explanted and tested for EpiSC growth (Fig. 3A,B). We analysed *Nanog*$^{-/-}$ cell lines TβC44cre6 and RCNβH-B(t), alongside a control derivative line RCNβH-B(t)R, in which one of the non-functional *Nanog* alleles has been repaired by homologous recombination (Chambers et al., 2007). Discrimination of ES cell-derived from wild-type host cells is possible because RCNβH-B(t) and RCNβH-B(t)R express GFP constitutively, whereas TβC44cre6 expresses GFP from a targeted *Nanog*-null allele. *Nanog*$^{-/-}$ cells formed chimaeras indistinguishable from wild-type or *Nanog*$^{-/+}$ cells (Fig. 3B). Explanted colonies of *Nanog*$^{-/-}$ cells were picked and expanded to produce two independent EpiSC lines that lacked Nanog but showed robust Oct4 and Sox2 expression (Fig. 3B; supplementary material Fig. S4A).

To exclude the formal possibility that initial derivation of chimaera-derived *Nanog*$^{-/-}$ lines required co-culture with wild-type cells, pure *Nanog*$^{-/-}$ ES cell populations were cultured in EpiSC conditions, previously shown to permit in vitro EpiSC derivation

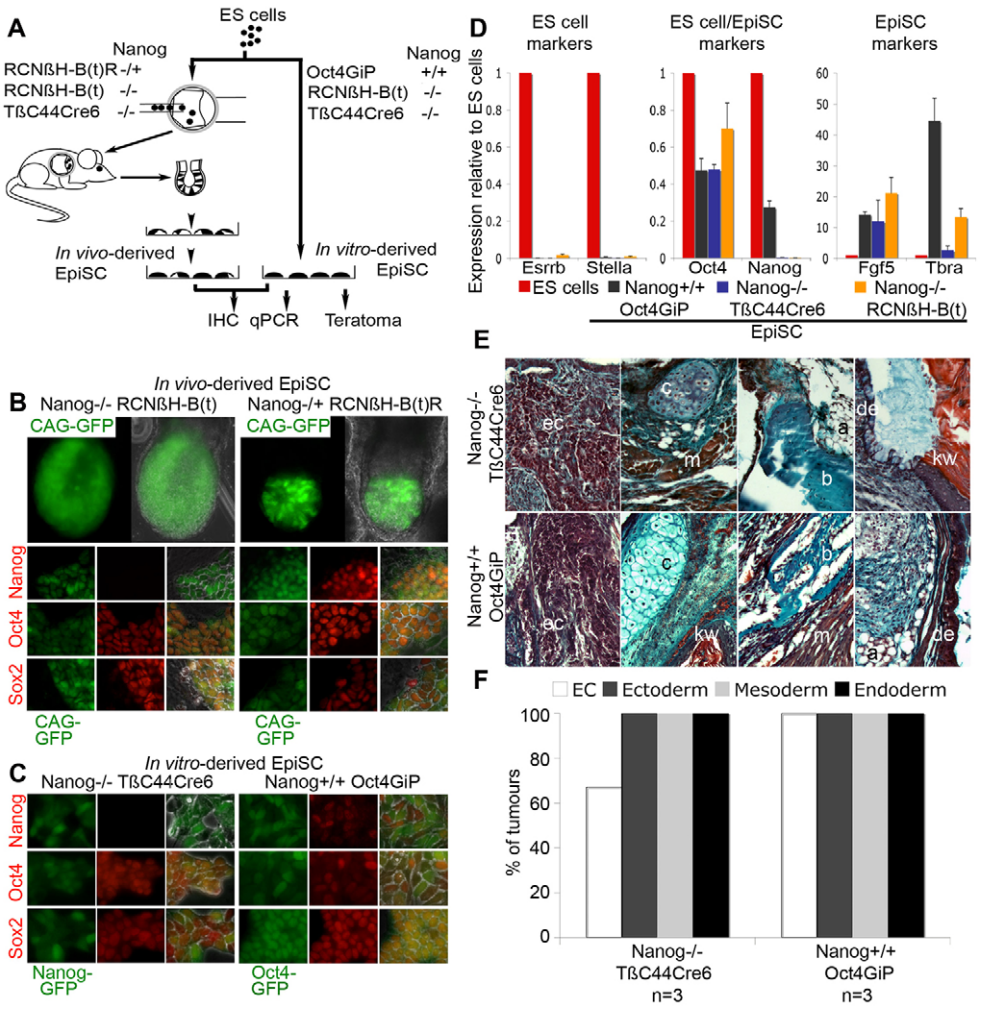

Fig. 3. Nanog is dispensable for EpiSC derivation and maintenance. (**A**) Experimental strategies for derivation and analysis of *Nanog*$^{-/-}$ EpiSC lines. The indicated *Nanog* mutant lines were analysed alongside *Nanog*$^{+/+}$ line Oct4GiP, carrying a GFP-ires-PuromycinR cassette expressed from the Oct4 promoter. IHC, immunohistochemistry. (**B**) Top: chimaeric embryos with *Nanog* mutant cells expressing constitutive GFP. Bottom: Oct4, Sox2 and Nanog immunofluorescence in EpiSC lines derived from chimaeric embryos. (**C**) ES cell lines derived directly in vitro from *Nanog*$^{-/-}$ and control lines. (**D**) mRNA expression of in in vitro-derived EpiSC lines. (**E**) Masson's trichrome-stained tumour sections derived from the indicated established EpiSC lines. ec, embryonal carcinoma cells; c, cartilage; m, skeletal muscle; b, bone; a, adipose; de, digestive epithelium; kw, keratin whorl. (**F**) Tumours in E scored for germ layer differentiation.

(Guo et al., 2009). Two independent in vitro-derived *Nanog*$^{-/-}$ EpiSC lines that expressed EpiSC-specific markers were readily obtained (Fig. 3C,D; supplementary material Fig. S4B). *Nanog*$^{-/-}$ EpiSC produced teratocarcinomas following kidney capsule grafting (Fig. 3E,F). Thus, in contrast to the necessity for Nanog in the acquisition of the 'ground state' pluripotency found in ES cells (Silva et al., 2009), Nanog is neither required to transit to nor to maintain EpiSC pluripotency, although Nanog expression marks both pluripotent states in vitro.

Previously, Nanog has been proposed as the key intermediary downstream of activin that is responsible for maintaining self-renewal of both human ES cells and mouse EpiSC (Vallier et al., 2009). However, as shown above, EpiSCs can be established and maintained without Nanog. To further investigate the signalling requirements of EpiSCs, epiblast tissue was explanted in the presence of signalling pathway inhibitors. In the presence of an activin inhibitor (but not a MEK/Erk inhibitor) epiblast tissue lost expression of Nanog:GFP (Fig. 4A). Moreover, similar to *Nanog*$^{+/-}$ Nanog: GFP explants, *Nanog*$^{-/-}$ EpiSC lines treated with activin inhibitor failed to maintain Nanog:GFP reporter expression at 48h (Fig. 4B,C). By contrast, *Nanog*$^{-/-}$ cells cultured in MEK/Erk inhibitor maintained Nanog:GFP expression at 48 hours. After 118 hours, Nanog:GFP expression and EpiSC morphology were lost in both conditions. Together, these results indicate that, in EpiSCs, Nanog is a target of activin signalling (Greber et al., 2010) but Nanog is not necessary for activin-dependent self-renewal (Vallier et al., 2009).

Role of Oct4 in post-implantation pluripotency

We next examined the spatiotemporal expression of Oct4. Until the late bud stage, Oct4 is widely expressed (Scholer et al., 1990; Yeom et al., 1996). However, from early headfold stage, levels of Oct4 mRNA and protein are consistently lower in the anterior part of the embryo containing the prospective forebrain, than more posterior regions (Fig. 5A,B) (Downs, 2008). Image analysis of Oct4 immunofluorescence shows a range of fluorescence intensity levels per nucleus, with consistently lower levels appearing in the anteriormost region at all headfold stages (Fig. 5C; supplementary material Fig. S5). Fluorescence intensity declined in both regions with increasing embryonic age (Fig. 5C). We tested Nanog reactivation in explanted tissue from two microdissected regions expressing different levels of Oct4: region 1 [low Oct4], corresponding to prospective forebrain, and the adjoining region 2 [higher Oct4] (Fig. 5C-F). The efficiency of Nanog reactivation in EpiSC culture was consistently lower in region 1 than region 2 through headfold stages (Fig. 5F). Moreover, the efficiency of Nanog-reactivation in both regions 1 and 2 declined with developmental stage (Fig. 5F) such that by early somitogenesis (zero to two somites) only an extremely low proportion of colonies expressed Nanog. Interestingly, the frequency of Nanog reactivation in each region at a given stage correlates with the frequency of cells showing immunofluorescence above a consistent threshold fluorescence intensity value (indicated by the dashed line in Fig. 5C), suggesting a minimum threshold of Oct4 for Nanog

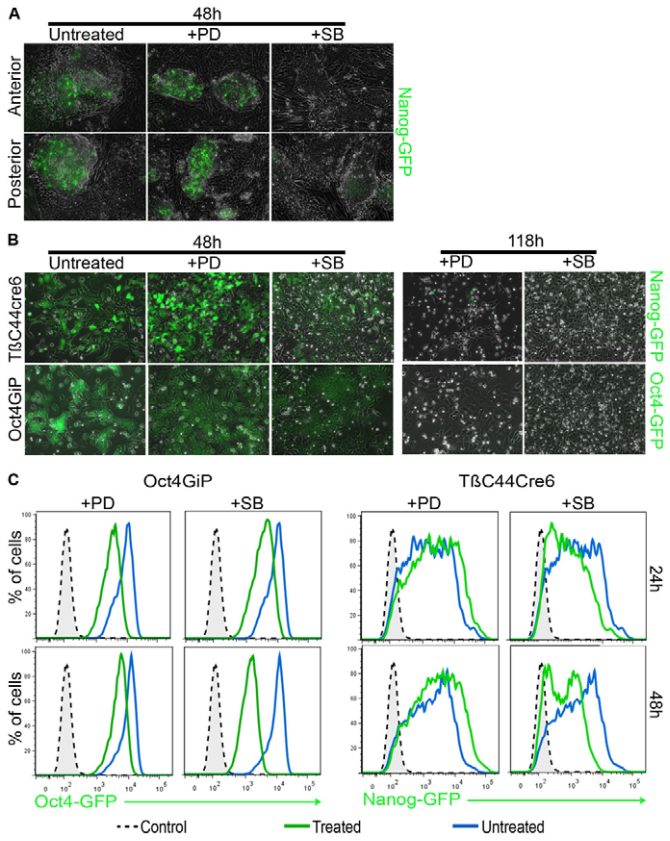

Fig. 4. The effect of activin on EpiSC derivation in the presence and absence of Nanog. (**A**) Colonies derived from anterior and posterior fragments of E7.5 embryos 48 hours after explantation showing Nanog:GFP expression in 10 μM SB431542 (SB) or 1 μM PD0325901 (PD). (**B**) Established *Nanog*$^{-/-}$ (TβC44cre6) and *Nanog*$^{+/+}$ (Oct4GiP, carrying an Oct4:GFP reporter) EpiSC lines treated with 10 μM SB431542 or 1 μM PD0325901 for 48 hours or 118 hours and examined by fluorescence and bright-field imaging. (**C**) FACS analysis of EpiSC lines examined in B at 24 and 48 hours. Control lines are wild-type EpiSC.

reactivation. The larger sample size at zero to two somites in these experiments compared with those in Fig. 2C bring increased resolution to the time period in which pluripotency is lost. Together, these data suggest that sufficiently high Oct4 levels may be important in embryonic pluripotency.

To determine the time over which this drop in Nanog reactivation occurs, we measured the duration of the headfold stage. Downs and Davies (Downs and Davies, 1993) and our independent observations indicate that late headfold stage embryos never constitute a majority of embryos dissected at 6-hourly intervals from E6.75-E8.25, suggesting that the duration of this stage is short (supplementary material Fig. S6). We cultured individually staged E6.5-E7.5 (late streak to late bud stage) embryos for 7-16 hours. All embryos developed according to the schedule expected from fresh dissections of embryos from timed matings (supplementary material Fig. S6A,C). This indicates that the culture conditions allow accurate reproduction of normal development over this period. Embryos cultured from early headfold stage developed to late headfold stage within 3 hours, and by 4 hours had formed one or two somites (n=3) (supplementary material Fig. S6B,C). Late headfold stage embryos had formed two or three somites within 4 hours (n=5) (supplementary material Fig. S6B,C). Therefore, the period of Oct4 downregulation critical to pluripotency loss at headfold stage is no longer than 4 hours.

To test the hypothesis that the reduction in Oct4 levels results in loss of embryonic pluripotency, the consequences of re-expressing Oct4 in somitogenesis-stage embryos were examined using mice carrying an Oct4 transgene (*TgOct4*) that is ubiquitously expressed in response to doxycycline administration (Hochedlinger et al., 2005). Explants from anterior (forebrain) and posterior (primitive streak) regions of somitogenesis-stage *TgOct4/+;rtTA/+* embryos up to E15.5 were tested for EpiSC colony formation and Nanog reactivation in the presence or absence of doxycycline (Fig. 6A). Doxycycline efficiently induced Oct4 expression, which was undetectable in untreated explants (Fig. 6B; supplementary material Fig. S7A). In explants from E8.5-E10.5, Nanog:GFP was induced in doxycycline-treated explants within 24 hours (Fig. 6B; supplementary material Fig. S7B) and both Nanog and Sox2 were robustly expressed by 48 hours (Fig. 6C; supplementary material Fig. S7C,E). Moreover, image analysis shows that Nanog is only reactivated in Oct4-expressing cells, confirming that Nanog reactivation is cell-autonomous (supplementary material Fig. S7D). Interestingly, cells with the highest intensity Oct4 immunofluorescence did not show Nanog reactivation, suggesting both a lower and upper threshold of Oct4 expression for optimal Nanog reactivation (supplementary material Fig. S7D). The majority (62%) of colonies expressed Nanog protein in 48-hour explants at E8.5 (n=68; Fig. 6B), and, of these, 25% of Oct4-expressing cells were Nanog protein-positive (n=11241; supplementary material Fig. S7D). The frequency of Nanog reactivation declined thereafter until E11.5 (3% of colonies; n=143) (Fig. 6B). At E13.5-E14.5, we observed no Nanog-positive colonies at 48 hours, but after a more prolonged period (120 hours) a few colonies had become Nanog positive (Fig. 6B). By E15.5, we found no Nanog-positive colonies in doxycycline-treated explants, even after 120 hours (Fig. 6B). Thus, Nanog reactivation in EpiSC culture is initially highly sensitive to raised Oct4 levels, but reactivation gradually becomes refractory to these conditions.

Despite the delay in reactivation of Nanog at E13.5, EpiSC lines expressing characteristic markers could be derived from embryos up to this stage (Fig. 6D,E; supplementary material Fig. S8A). A total of 34 E9.0-E13.5 EpiSC lines have been established and passaged up to 30 times (supplementary material Table S1). As seen in presomite stage EpiSC lines, marker gene expression levels varied (Fig. 6E), but were within the range of previously reported expression levels (Brons et al., 2007; Guo and Smith, 2010; Guo et al., 2009; Hayashi and Surani, 2009). Crucially, a representative E10.5 EpiSC line showed activin and MEK/ERK-dependent, Jak/STAT signalling-independent propagation (supplementary material Fig. S9). Moreover, teratocarcinoma-forming capacity was retained after prolonged culture in the presence of a Jak inhibitor (Fig. 6F; supplementary material Fig. S8B). To detect the presence of self-renewing cells in the tumour, secondary EpiSC were isolated. After four passages, these lines showed characteristic EpiSC morphology and expressed Oct4, Nanog and Sox (supplementary material Fig. S8C). To test whether Oct4 induces teratocarcinoma-forming potential without prior EpiSC line establishment, freshly dissected *TgOct4/+;rtTA/+* E8.5 (five- to 11-somite stage) forebrain regions were grafted to the kidney capsule of wild-type hosts. Graft recipient animals were maintained with or without doxycycline (Fig. 6F). After 4 weeks, two out of three doxycycline-treated grafts had formed large teratocarcinomas containing derivatives of all three germ layers (Fig. 6F;

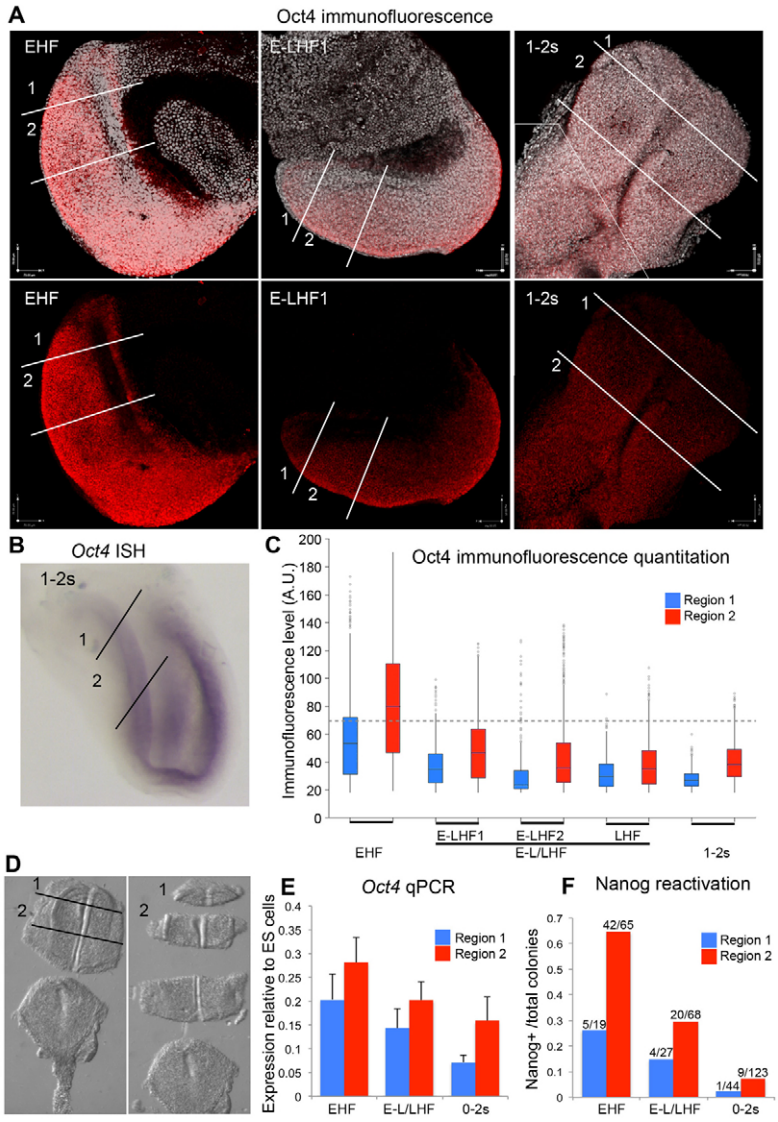

Fig. 5. Oct4 levels in the pre-somitogenesis epiblast correlate with efficiency of Nanog reactivation. (**A**) Confocal *z*-stack showing immunohistochemical analysis of anterior Oct4 expression in early headfold (EHF), early to late headfold (E-LHF) and one- to two-somite (1-2s) stage embryos. Top row: overlay of Oct4 protein immunofluorescence (red) with DAPI (grey). Lines indicate analysed regions 1 and 2. Bottom row: Oct4 protein. (**B**) Whole-mount in situ hybridization of *Oct4* mRNA levels in a one- to two-somite embryo. Positions of regions 1 and 2 are indicated by lines. (**C**) Box-whisker plot showing the distribution of Oct4 immunofluorescence above background of regions 1 and 2 in five embryos from headfold to early somite stage (see supplementary material Fig. S5 for the regions analysed). Boxes define limits of the upper and lower 25% of values (Q3-Q1). Horizontal line indicates the median value. Vertical lines (whiskers) represent 1.5×(Q3-Q1). Dots indicates individual outliers of intensity greater than 1.5×(Q3-Q1). Pearson product-moment correlation coefficient analysis examining the linear 'fit' of the relationship between the fraction of nuclei above a threshold immunofluorescence level in each region, and the percentage of Nanog-reactivating colonies, reveals a maximum at 66 average pixel intensity unit values (A.U; R^2=0.92; dotted line). (**D**) Microdissection of regions 1 and 2 from a one- to two-somite embryo. (**E**) *Oct4* mRNA expression in pooled samples of regions 1 and 2 microdissected from embryos of the indicated stages. Data are mean±s.e.m. (**F**) Frequency of Nanog immunofluorescent colonies from regions 1 and 2, isolated from pooled embryos of the indicated stages and explanted in EpiSC conditions for 48 hours. Number of Nanog$^+$ colonies/total scored is indicated.

supplementary material Fig. S8B), whereas untreated tissue formed only small, differentiated tumours. Taken together, these results indicate that threshold levels of Oct4 are necessary to maintain pluripotency in the presomitogenesis embryo, as well as to mediate its re-acquisition in somitogenesis-stage, non-pluripotent cells.

Changes in nucleosome occupancy accompany the loss and reacquisition of pluripotency

To investigate whether the loss and reacquisition of pluripotency is underpinned by chromatin changes, we examined nucleosome positioning at the regulatory regions of Oct4 and Nanog (Fig. 7A). Analysis of nucleosome-depleted chromatin using formaldehyde assisted isolation of regulatory elements (FAIRE) (Giresi et al., 2007) showed prominent changes between presomite and early somite stages. Despite the mixture of cell types (including those expressing low level Oct4 and Nanog) present in embryos at these stages, we detected a profound reduction in the overall accessibility of chromatin at both *Oct4* and *Nanog* regulatory regions in whole embryos (Fig. 7B), correlating with the observed changes in transcript levels. This chromatin closure was reversed in two- to eight-somite stage Oct4-expressing explants after 24 hours in EpiSC culture (Fig. 7C). Although both *Nanog* and *Oct4* chromatin reopened following Oct4 induction, *Oct4* regulatory elements did not show as extensive reopening as *Nanog* (Fig. 7C). This is noteworthy given that *Nanog* expression is extinguished prior to *Oct4* and suggests that genes of the pluripotency network do not all recover simultaneously. Moreover, activin/FGF culture conditions alone can provoke chromatin reopening at *Nanog* in the absence of ectopic Oct4 expression and Nanog reactivation (Fig. 7C). This suggests that activin/FGF can stimulate nucleosomal displacement at the *Nanog* promoter but that binding of Oct4 to the Oct/Sox motif is required to stimulate *Nanog* transcription.

Progressive decline in pluripotency reactivation correlates with increased methylation at *Nanog*

The failure to reactivate Nanog in post-pluripotent tissue and the decreasing efficiency of reactivation in presence of elevated Oct4 expression suggested that progressive stabilizing changes may occur at *Nanog*. We therefore examined the extent of CpG methylation in E7.5-E14.5 embryos at the Nanog promoter (Fig. 7D). This region has been shown to exhibit much higher levels of methylation in MEFs compared with embryonic stem cells (Imamura et al., 2006). We found that methylation levels were low at both presomite and early somite stages (Fig. 7D), but increased

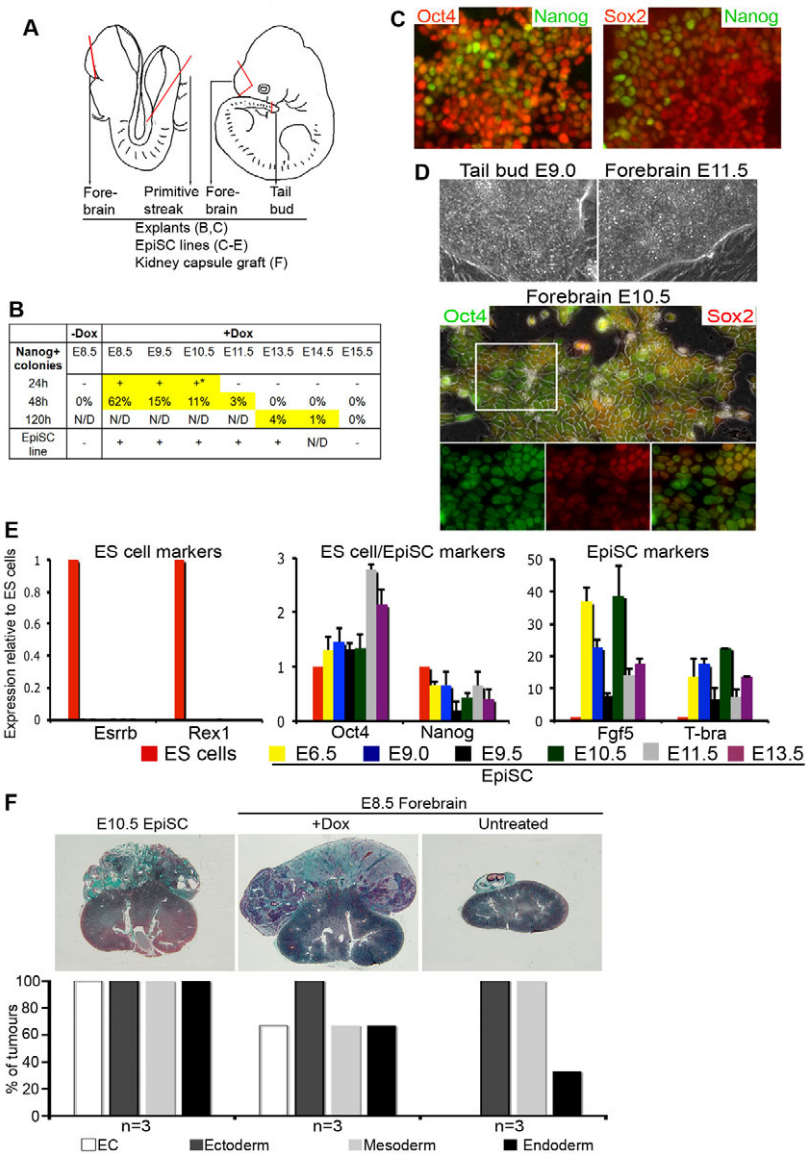

Fig. 6. Oct4 mediates Nanog reactivation and pluripotency in somitogenesis-stage embryo explants. (**A**) Schematic diagram showing regions dissected and assays performed. (**B**) Scoring of Nanog-positive colonies from explanted *TgOct4/+;rtTA/+* forebrain regions of the indicated stage embryos cultured in the presence or absence of doxycycline. Successful (+) or unsuccessful (–) EpiSC line derivation at each stage is indicated. Asterisk indicates only one Nanog-positive colony was observed after 24 hours. N/D, not determined. Number of colonies scored: E8.5+Dox, *n*=68; E8.5-Dox, *n*=53; E9.5, *n*=648; E10.5, *n*=675; E11.5, *n*=143; E13.5, *n*=220; E14.5-48 hours, *n*=283; E14.5-120 hours, *n*=428; E15.5-48 hours, *n*=145; E15.5-120 hours, *n*=660. (**C**) Nanog and Oct4 or Sox2 immunofluorescence in E8.5 and E9.5 forebrain explants. (**D**) Established EpiSC lines. Top: bright-field images showing morphology of representative lines. Bottom: Oct4 and Sox2 immunofluorescence. Box indicates the region magnified below. (**E**) mRNA expression in established EpiSC lines derived from the indicated embryonic stages. Data are mean±s.e.m. (**F**) Teratocarcinoma formation by an established EpiSC line derived from E10.5 forebrain and cultured for 1 month in Jak inhibitor I, and by freshly dissected forebrain explants transplanted to untreated and doxycycline-treated mice. Grafts were scored for germ layer differentiation. The presence of endodermal tissues in one of the latter tumours may result from inclusion of anterior foregut in the dissected tissue.

as development progressed. Moreover, analysis of an established EpiSC line derived from E13.5 Oct4-overexpressing forebrain tissue showed that DNA methylation levels at the *Nanog* promoter resemble those of pre-somite E7.5 embryos (Fig. 7D). These findings show that Oct4-induced *Nanog* reactivation and acquisition of pluripotency in somitogenesis-stage explants is accompanied by lowered methylation at *Nanog*, whereas the progressive decrease in its efficiency late in development correlates with increasing *Nanog* promoter methylation.

DISCUSSION

Here, we examine the role of two core pluripotency factors, Nanog and Oct4, in pluripotency during post-implantation development. We show that Nanog expression in vitro is a reliable indicator of pluripotency but is dispensable for the maintenance of post-implantation pluripotency. We have identified a novel transition state when cells are no longer pluripotent but can rapidly reacquire pluripotency upon re-expression of Oct4. Our work suggests that two mechanisms operate to ensure that pluripotent cells are eliminated from the somitogenesis-stage embryo. The first is a rapid chromatin-based shutdown that is susceptible to perturbation by variation in the levels of pluripotency network components, and the second is a slower, more permanent, DNA methylation-based stabilization of the non-pluripotent state (Fig. 7E).

Nanog-independent EpiSC self-renewal

The ability of Nanog-null epiblast cells to form EpiSCs rigorously establishes that Nanog is neither a necessary mediator of activin signalling in EpiSC, nor is it required for EpiSC maintenance or derivation. Interestingly, established ES cell lines, which also have no absolute requirement for Nanog, nevertheless show decreased self-renewal efficiency in the absence of Nanog (Chambers et al., 2007). Whether similar quantitative effects of Nanog on self-renewal or differentiation of EpiSCs exist remains an unanswered question.

Induction of pluripotency in somatic cells in vivo

The efficient reactivation of pluripotency in the time window between the onset of somitogenesis (E8.0) and late organogenesis (E10.5) following re-expression of Oct4 demonstrates that pluripotency, and therefore teratocarcinogenesis, could result from the reactivation of expression of a single gene during this time.

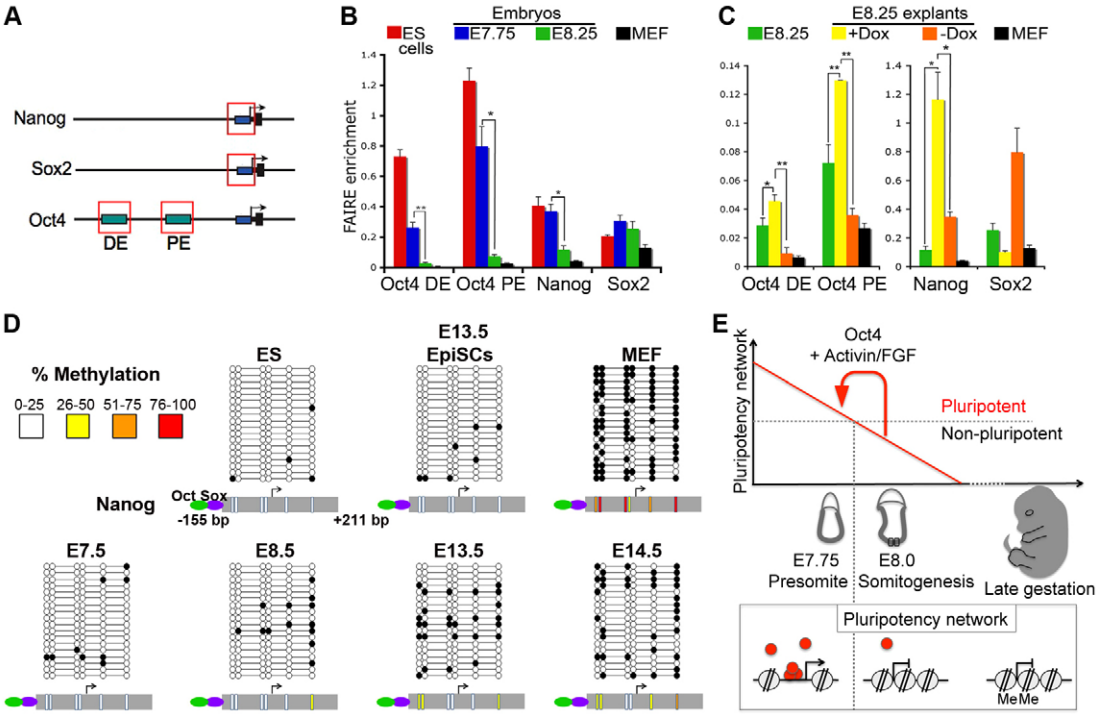

Fig. 7. Chromatin changes at pluripotency transcription factor genes. (**A**) Schematic diagram showing the analysed regions (boxed) of the *Nanog* and *Sox2* promoters and the distal enhancer (DE) and proximal enhancer (PE) of *Oct4*. Arrow indicates transcriptional start site (TSS). (**B**) FAIRE enrichment (ratio of test:reference DNA, normalized to β-actin) of pluripotency transcription factor genes in presomite (LB-EHF; E7.75) and somitogenesis-stage (two to eight somites; E8.25) embryos compared with ES cells and MEFs. Significant differences in C and D, established by *t*-test: **P*>0.05; ***P*>0.01. Data are mean±s.e.m. (**C**) FAIRE of E8.25 embryo explants cultured for 24 hours in EpiSC conditions in the presence (+Dox) or absence (–Dox) of doxycycline compared with E8.25 tissue or MEFs. Data are mean±s.e.m. (**D**) Methylation analysis of the Nanog proximal region (grey rectangle) by bisulphite sequencing of DNA extracted from whole embryos at the indicated stages. Methylation levels in ES cells, MEFs and an established E13.5 forebrain EpiSC line are shown for comparison. Filled (methylated) or empty (unmethylated) circles: CpGs on individual DNA molecules (horizontal lines). Below each stage, vertical bars superimposed on the *Nanog* promoter represent the proportion of methylated CpGs at each position. Green/purple ovals indicate Oct/Sox-binding sites. Arrows indicate the transcriptional start site (TSS). (**E**) Model. Levels of pluripotency gene regulatory network activity (red) decline during post-implantation development, reaching a threshold at the onset of somitogenesis where levels become too low to sustain pluripotency. Decreased accessibility of regulatory elements due to nucleosome invasion extinguish pluripotency. Elevation of Oct4 in co-operation with activin/FGF, is sufficient to revive the pluripotent state, whereas methylation stabilizes the non-pluripotent state.

Reactivation of Oct4 in 3-week-old animals does not result in teratocarcinoma formation (Hochedlinger et al., 2005), suggesting that the competence of cells to respond to elevated Oct4 by re-establishing the pluripotent state is limited to earlier stages. E8-E10 in mouse corresponds approximately to human Carnegie stages 9-14 (20-33 days post ovulation) (Kaufman, 1992). Such an early developmental origin for human neonatal teratomas would be consistent with the occasionally very large size of such tumours and appearance in ultrasound scans as early as 13.5 weeks in human foetuses (Holcroft et al., 2008). The efficient formation of teratocarcinomas from primary somatic tissue in mouse, which has been unambiguously separated from locations occupied by PGCs, indicates that a somatic origin for these tumours in humans is possible. This therefore calls into question the prevailing notion that human extragonadal teratocarcinomas have an obligatory origin from misplaced PGCs (Oosterhuis and Looijenga, 2005).

Distinction between reprogramming and reactivation of pluripotency

The window of rapid and efficient reactivation of pluripotency is qualitatively distinct from other reports of reprogramming differentiated cells to pluripotency. Oct4-induced reprogramming to pluripotency has been achieved for a variety of cell types (Kim et al., 2009a; Kim et al., 2009b; Tsai et al., 2011). However, these reprogramming processes take a minimum of 18 days (Tsai et al., 2011). This difference cannot be explained by the time taken to generate iPS cells rather than EpiSC, as generation of iEpiSC from mouse embryonic fibroblasts using Oct4, Myc, Klf4 and Sox2 together only occurs after 2 weeks and only exceeds iPS cell efficiency by a factor of 4 (Han et al., 2011). This reinforces the conclusion that the E8.0-E10.5 stage marks a distinct transition state prior to the stable shutdown of pluripotency.

Progressive dismantling of the pluripotency gene regulatory network

We observe that Oct4 and Nanog levels are reduced in early post-implantation embryos compared with ES cells, and decline further during post-implantation development. Furthermore, several transcription factors (e.g. Esrrb, Klf4 that are thought to function combinatorially with Oct4, Sox2 and Nanog in ES cells and in pre-implantation embryos, are downregulated during post-implantation development (Han et al., 2010). Interestingly, the period from bud stage to early somitogenesis is characterized by the downregulation of many pluripotency associated genes (Mitiku and Baker, 2007).

The regionalization of Nanog and Oct4 during gastrulation further points to a progressive dismantling of the pluripotency network. We observe a rapid loss of pluripotency, in under 4 hours, in cells where Oct4 protein levels are diminishing but still present, suggesting that threshold concentrations of this factor, rather than its absolute presence, determine pluripotency. Therefore, the gradual decrease in expression levels of individual pluripotency transcription factors may be rapidly converted into dramatic chromatin condensation at pluripotency gene regulatory elements over a short developmental period. This could manifest itself as a sudden collapse in the overall activity of the pluripotency gene regulatory network and, consequently, of pluripotency.

The disappearance of nucleosome-depleted regions may be an effect of this reduction in pluripotency factor concentrations, but could also result from an increase in histone modifications associated with repression. The observation that both distal and proximal Oct4 enhancers and the Nanog promoter show chromatin opening following Oct4 transgene induction is consistent with the observations that Oct4 binds these regulatory regions in EpiSCs (Tesar et al., 2007). However, the accessibility of chromatin at the Nanog promoter also increases after explantation without Oct4 induction, when Nanog is not expressed. This suggests that chromatin re-opening is not simply a consequence of transcriptional activity, nor is it obligatorily linked to an increase in Oct4 concentration. The apparent increase in accessibility of the Sox2 promoter in activin/FGF in the absence of Oct4 induction may reflect its activity in neural progenitors, as Fgf2 can promote the growth of neural stem cells from embryos of this stage (Tropepe et al., 1999).

Our results demonstrate that nucleosome depletion at the Nanog proximal promoter is a crucial readout of a pluripotent state. Our finding that increased nucleosome occupancy at the *Nanog* promoter is reversible by increased Oct4 expression is interesting in light of the recent report that Oct4 binding maintains a nucleosomes-depleted region at the *Nanog* promoter in human EC cells (You et al., 2011). This study provides evidence that enforcing Oct4 expression in differentiated cancer cell lines restored regions of nucleosome depletion but only in the absence of DNA methylation. The same study reported that increased nucleosome occupancy during EC differentiation precedes DNA methylation, which also inhibits restoration of nucleosomes-depleted regions by forced Oct4 expression. Our data show that similar events occur in the more physiological context of mouse embryogenesis. This offers a potential explanation for the decreasing ability of enforced Oct4 expression to resuscitate pluripotency in explanted tissue and support a model in which the long-term stabilization of *Nanog* suppression is achieved by progressively increasing levels of methylation at *Nanog* between E8.5 and E15.5.

Significance of pluripotency factor expression in vivo

The high levels of Nanog in the proximal/posterior part of the epiblast, together with its disappearance on E7.5 and the remnant of expression in the node coincide with areas of Nodal expression and suggest that, just as in EpiSCs, Nanog expression is induced by Nodal/activin signalling in the post-implantation embryo. Thus, the presence of Nodal antagonists in the anterior visceral endoderm, which restrict Nodal signalling to the posterior of the embryo (Perea-Gomez et al., 2002), may also restrict Nanog to the proximal/posterior region. On dispersal of cells at explantation, the endoderm and epiblast separate, and thus in EpiSC culture conditions, epiblast cells are removed from Nodal antagonists and subjected to more uniform activin signalling. This could account for the rapid reactivation of Nanog in presomitic distal/anterior explants and the ability of inhibitors of activin/Nodal signalling to block reactivation in anterior explants.

During somitogenesis, when pluripotency has been extinguished from the epiblast, FGF and Nodal are used for organ-specific patterning roles. For example, Fgf8 patterns the mid/hindbrain junction (Crossley et al., 1996), while Nodal directs left/right asymmetry (Kawasumi et al., 2011). These events may dictate that by early somitogenesis stage the activation of the pluripotency network as a response to Nodal and FGF signalling is detrimental, and therefore requires efficient shutdown just prior to organogenesis.

It is likely that activity of the pluripotency network is not required by E7.5, as cell fates at this stage are highly regionalized. In particular, the region corresponding to Nanog-negative anterior epiblast is exclusively fated for neurectoderm (Forlani et al., 2003; Lawson et al., 1991; Lawson and Pedersen, 1992). The fact that these cells retain pluripotency and reactivate Nanog upon explantation indicates plasticity in gene expression during this pre-commitment stage coupled to an ability to reassert the activity of the pluripotency gene regulatory network upon appropriate environmental alteration represented by activin/FGF. This plasticity is lost at the onset of somitogenesis and marks the natural end of pluripotency at a time when Oct4 levels are continuing to decline. The subsequent resuscitation of pluripotency by the activation of a single transcription factor establishes that critical commitment events can hinge on modest changes in the activity of a single gene product, in this case, Oct4.

Acknowledgements

We thank John Agnew, Douglas Colby, Carolyn Manson, Renée McLay, Lynsey Robertson, Frances Stenhouse and Jan Ure, for technical assistance, and Clare Blackburn, Josh Brickman, Huw Jones, Keisuke Kaji, Pablo Navarro and Jenny Nichols for comments on the manuscript.

Funding

This research was supported by funding from the EU Framework 7 project 'EuroSyStem' and The Wellcome Trust [WT073607/Z/03/Z to I.C.], by the UK Medical Research Council [G091533 to I.C. and G080297 to V.W.], by the Association for International Cancer Research [08-0493 to V.W.] and by a studentship from CONACYT (to R.O.). Deposited in PMC for release after 6 months.

Competing interests statement

The authors declare no competing financial interests.

Supplementary material

Supplementary material available online at
http://dev.biologists.org/lookup/suppl/doi:10.1242/dev.078071/-/DC1

References

Andrews, P. W. (2002). From teratocarcinomas to embryonic stem cells. *Philos. Trans. R. Soc. Lond. B Biol. Sci.* **357**, 405-417.

Avilion, A. A., Nicolis, S. K., Pevny, L. H., Perez, L., Vivian, N. and Lovell-Badge, R. (2003). Multipotent cell lineages in early mouse development depend on SOX2 function. *Genes Dev.* **17**, 126-140.

Bancroft, J. and Gamble, M. (2002). *Theory and Practice of Histological Techniques.* London: Churchill Livingstone.

Beddington, R. S. (1983). Histogenetic and neoplastic potential of different regions of the mouse embryonic egg cylinder. *J. Embryol. Exp. Morphol.* **75**, 189-204.

Brons, I. G., Smithers, L. E., Trotter, M. W., Rugg-Gunn, P., Sun, B., Chuva de Sousa Lopes, S. M., Howlett, S. K., Clarkson, A., Ahrlund-Richter, L., Pedersen, R. A. et al. (2007). Derivation of pluripotent epiblast stem cells from mammalian embryos. *Nature* **448**, 191-195.

Cambray, N. and Wilson, V. (2007). Two distinct sources for a population of maturing axial progenitors. *Development* **134**, 2829-2840.

Chambers, I. (2004). Mechanisms and factors in embryonic stem cell self-renewal. *Rend. Fis. Acc. Lincei* **16**, 83-97.

Chambers, I. and Tomlinson, S. R. (2009). The transcriptional foundation of pluripotency. *Development* **136**, 2311-2322.
Chambers, I., Colby, D., Robertson, M., Nichols, J., Lee, S., Tweedie, S. and Smith, A. (2003). Functional expression cloning of Nanog, a pluripotency sustaining factor in embryonic stem cells. *Cell* **113**, 643-655.
Chambers, I., Silva, J., Colby, D., Nichols, J., Nijmeijer, B., Robertson, M., Vrana, J., Jones, K., Grotewold, L. and Smith, A. (2007). Nanog safeguards pluripotency and mediates germline development. *Nature* **450**, 1230-1234.
Copp, A. J. (1990). Dissection and culture of postimplantation embryos. In *Postimplantation Development in the Mouse: A Practical Approach* (ed. A. J. Copp and D. L. Cockroft), pp. 15-40. Oxford: IRL Press.
Crossley, P. H., Martinez, S. and Martin, G. R. (1996). Midbrain development induced by FGF8 in the chick embryo. *Nature* **380**, 66-68.
Damjanov, I., Solter, D. and Skreb, N. (1971). Teratocarcinogenesis as related to the age of embryos grafted under the kidney capsule. *Roux's Arch. Dev. Biol.* **167**, 288-290.
Downs, K. M. (2008). Systematic localization of Oct-3/4 to the gastrulating mouse conceptus suggests manifold roles in mammalian development. *Dev. Dyn.* **237**, 464-475.
Downs, K. M. and Davies, T. (1993). Staging of gastrulating mouse embryos by morphological landmarks in the dissecting microscope. *Development* **118**, 1255-1266.
Forlani, S., Lawson, K. A. and Deschamps, J. (2003). Acquisition of Hox codes during gastrulation and axial elongation in the mouse embryo. *Development* **130**, 3807-3819.
Giresi, P. G., Kim, J., McDaniell, R. M., Iyer, V. R. and Lieb, J. D. (2007). FAIRE (Formaldehyde-Assisted Isolation of Regulatory Elements) isolates active regulatory elements from human chromatin. *Genome Res.* **17**, 877-885.
Greber, B., Wu, G., Bernemann, C., Joo, J. Y., Han, D. W., Ko, K., Tapia, N., Sabour, D., Sterneckert, J., Tesar, P. et al. (2010). Conserved and divergent roles of FGF signaling in mouse epiblast stem cells and human embryonic stem cells. *Cell Stem Cell* **6**, 215-226.
Guo, G. and Smith, A. (2010). A genome-wide screen in EpiSCs identifies Nr5a nuclear receptors as potent inducers of ground state pluripotency. *Development* **137**, 3185-3192.
Guo, G., Yang, J., Nichols, J., Hall, J. S., Eyres, I., Mansfield, W. and Smith, A. (2009). Klf4 reverts developmentally programmed restriction of ground state pluripotency. *Development* **136**, 1063-1069.
Han, D. W., Tapia, N., Joo, J. Y., Greber, B., Arauzo-Bravo, M. J., Bernemann, C., Ko, K., Wu, G., Stehling, M., Do, J. T. et al. (2010). Epiblast stem cell subpopulations represent mouse embryos of distinct pregastrulation stages. *Cell* **143**, 617-627.
Han, D. W., Greber, B., Wu, G., Tapia, N., Arauzo-Bravo, M. J., Ko, K., Bernemann, C., Stehling, M. and Scholer, H. R. (2011). Direct reprogramming of fibroblasts into epiblast stem cells. *Nat. Cell Biol.* **13**, 66-71.
Hart, A. H., Hartley, L., Ibrahim, M. and Robb, L. (2004). Identification, cloning and expression analysis of the pluripotency promoting Nanog genes in mouse and human. *Dev. Dyn.* **230**, 187-198.
Hatano, S. Y., Tada, M., Kimura, H., Yamaguchi, S., Kono, T., Nakano, T., Suemori, H., Nakatsuji, N. and Tada, T. (2005). Pluripotential competence of cells associated with Nanog activity. *Mech. Dev.* **122**, 67-79.
Hayashi, K. and Surani, M. A. (2009). Self-renewing epiblast stem cells exhibit continual delineation of germ cells with epigenetic reprogramming in vitro. *Development* **136**, 3549-3556.
Hochedlinger, K., Yamada, Y., Beard, C. and Jaenisch, R. (2005). Ectopic expression of Oct-4 blocks progenitor-cell differentiation and causes dysplasia in epithelial tissues. *Cell* **121**, 465-477.
Holcroft, C. J., Blakemore, K. J., Gurewitsch, E. D., Driggers, R. W., Northington, F. J. and Fischer, A. C. (2008). Large fetal sacrococcygeal teratomas: could early delivery improve outcome? *Fetal Diagn. Ther.* **24**, 55-60.
Imamura, M., Miura, K., Iwabuchi, K., Ichisaka, T., Nakagawa, M., Lee, J., Kanatsu-Shinohara, M., Shinohara, T. and Yamanaka, S. (2006). Transcriptional repression and DNA hypermethylation of a small set of ES cell marker genes in male germline stem cells. *BMC Dev. Biol.* **6**, 34.
Kaufman, M. (1992). *The Atlas of Mouse Development.* London: Academic Press.
Kawasumi, A., Nakamura, T., Iwai, N., Yashiro, K., Saijoh, Y., Belo, J. A., Shiratori, H. and Hamada, H. (2011). Left-right asymmetry in the level of active Nodal protein produced in the node is translated into left-right asymmetry in the lateral plate of mouse embryos. *Dev. Biol.* **353**, 321-330.
Kim, J. B., Greber, B., Arauzo-Bravo, M. J., Meyer, J., Park, K. I., Zaehres, H. and Scholer, H. R. (2009a). Direct reprogramming of human neural stem cells by OCT4. *Nature* **461**, 649-653.
Kim, J. B., Sebastiano, V., Wu, G., Arauzo-Bravo, M. J., Sasse, P., Gentile, L., Ko, K., Ruau, D., Ehrich, M., van den Boom, D. et al. (2009b). Oct4-induced pluripotency in adult neural stem cells. *Cell* **136**, 411-419.
Lawson, K. A. and Pedersen, R. A. (1992). Clonal analysis of cell fate during gastrulation and early neurulation in the mouse. *Ciba Found Symp.* **165**, 3-21; discussion 21-26.
Lawson, K. A., Meneses, J. J. and Pedersen, R. A. (1991). Clonal analysis of epiblast fate during germ layer formation in the mouse embryo. *Development* **113**, 891-911.
Li, G., Liu, T., Tarokh, A., Nie, J., Guo, L., Mara, A., Holley, S. and Wong, S. T. (2007). 3D cell nuclei segmentation based on gradient flow tracking. *BMC Cell Biol.* **8**, 40.
Masui, S., Nakatake, Y., Toyooka, Y., Shimosato, D., Yagi, R., Takahashi, K., Okochi, H., Okuda, A., Matoba, R., Sharov, A. A. et al. (2007). Pluripotency governed by Sox2 via regulation of Oct3/4 expression in mouse embryonic stem cells. *Nat. Cell Biol.* **9**, 625-635.
Mitiku, N. and Baker, J. C. (2007). Genomic analysis of gastrulation and organogenesis in the mouse. *Dev. Cell* **13**, 897-907.
Mitsui, K., Tokuzawa, Y., Itoh, H., Segawa, K., Murakami, M., Takahashi, K., Maruyama, M., Maeda, M. and Yamanaka, S. (2003). The homeoprotein Nanog is required for maintenance of pluripotency in mouse epiblast and ES cells. *Cell* **113**, 631-642.
Navarro, P., Moffat, M., Mullin, N. P. and Chambers, I. (2010). The X-inactivation trans-activator Rnf12 is negatively regulated by pluripotency factors in embryonic stem cells. *Hum. Genet.* **130**, 255-264.
Nichols, J., Zevnik, B., Anastassiadis, K., Niwa, H., Klewe-Nebenius, D., Chambers, I., Scholer, H. and Smith, A. (1998). Formation of pluripotent stem cells in the mammalian embryo depends on the POU transcription factor Oct4. *Cell* **95**, 379-391.
Niwa, H., Miyazaki, J. and Smith, A. G. (2000). Quantitative expression of Oct-3/4 defines differentiation, dedifferentiation or self-renewal of ES cells. *Nat. Genet.* **24**, 372-376.
Oosterhuis, J. W. and Looijenga, L. H. (2005). Testicular germ-cell tumours in a broader perspective. *Nat. Rev. Cancer* **5**, 210-222.
Perea-Gomez, A., Vella, F. D., Shawlot, W., Oulad-Abdelghani, M., Chazaud, C., Meno, C., Pfister, V., Chen, L., Robertson, E., Hamada, H. et al. (2002). Nodal antagonists in the anterior visceral endoderm prevent the formation of multiple primitive streaks. *Dev. Cell* **3**, 745-756.
Scholer, H. R., Dressler, G. R., Balling, R., Rohdewohld, H. and Gruss, P. (1990). Oct-4: a germline-specific transcription factor mapping to the mouse t-complex. *EMBO J.* **9**, 2185-2195.
Silva, J., Nichols, J., Theunissen, T. W., Guo, G., van Oosten, A. L., Barrandon, O., Wray, J., Yamanaka, S., Chambers, I. and Smith, A. (2009). Nanog is the gateway to the pluripotent ground state. *Cell* **138**, 722-737.
Solter, D. (2006). From teratocarcinomas to embryonic stem cells and beyond: a history of embryonic stem cell research. *Nat. Rev. Genet.* **7**, 319-327.
Tam, P. P. (1990). Studying development in embryo fragments. In *Postimplantation Mammalian Embryos, A Practical Approach* (ed. A. J. Copp and D. L. Cockroft), pp. 317-336. Oxford: IRL Press.
Tesar, P. J., Chenoweth, J. G., Brook, F. A., Davies, T. J., Evans, E. P., Mack, D. L., Gardner, R. L. and McKay, R. D. (2007). New cell lines from mouse epiblast share defining features with human embryonic stem cells. *Nature* **448**, 196-199.
Tropepe, V., Sibilia, M., Ciruna, B. G., Rossant, J., Wagner, E. F. and van der Kooy, D. (1999). Distinct neural stem cells proliferate in response to EGF and FGF in the developing mouse telencephalon. *Dev. Biol.* **208**, 166-188.
Tsai, S. Y., Bouwman, B. A., Ang, Y. S., Kim, S. J., Lee, D. F., Lemischka, I. R. and Rendl, M. (2011). Single transcription factor reprogramming of hair follicle dermal papilla cells to induced pluripotent stem cells. *Stem Cells* **29**, 964-971.
Vallier, L., Mendjan, S., Brown, S., Chng, Z., Teo, A., Smithers, L. E., Trotter, M. W., Cho, C. H., Martinez, A., Rugg-Gunn, P. et al. (2009). Activin/Nodal signalling maintains pluripotency by controlling Nanog expression. *Development* **136**, 1339-1349.
Wilkinson, D. G., Bhatt, S. and Herrmann, B. G. (1990). Expression pattern of the mouse T gene and its role in mesoderm formation. *Nature* **343**, 657-659.
Yamaguchi, S., Kimura, H., Tada, M., Nakatsuji, N. and Tada, T. (2005). Nanog expression in mouse germ cell development. *Gene Expr. Patterns* **5**, 639-646.
Yeom, Y. I., Fuhrmann, G., Ovitt, C. E., Brehm, A., Ohbo, K., Gross, M., Hubner, K. and Scholer, H. R. (1996). Germline regulatory element of Oct-4 specific for the totipotent cycle of embryonal cells. *Development* **122**, 881-894.
Ying, Q. L., Nichols, J., Evans, E. P. and Smith, A. G. (2002). Changing potency by spontaneous fusion. *Nature* **416**, 545-548.
You, J. S., Kelly, T. K., De Carvalho, D. D., Taberlay, P. C., Liang, G. and Jones, P. A. (2011). OCT4 establishes and maintains nucleosome-depleted regions that provide additional layers of epigenetic regulation of its target genes. *Proc. Natl. Acad. Sci. USA* **108**, 14497-14502.